Proc. Natl. Acad. Sci. USA
Vol. 93, pp. 9594–9599, September 1996
Cell Biology

Altered surfactant function and structure in SP-A gene targeted mice

THOMAS R. KORFHAGEN*†, MICHAEL D. BRUNO*, GARY F. ROSS*, KAREN M. HUELSMAN*, MACHIKO IKEGAMI‡, ALAN H. JOBE‡, SUSAN E. WERT*, BARRY R. STRIPP*§, RANDAL E. MORRIS*, STEPHAN W. GLASSER*, CINDY J. BACHURSKI*, HARRIET S. IWAMOTO*, AND JEFFREY A. WHITSETT*

*Children's Hospital Medical Center, Department of Pediatrics, Cincinnati, OH 45229-3039; and ‡Department of Pediatrics, Harbor–University of California, Los Angeles, Medical Center, Torrance, CA 90509

Communicated by John A. Clements, University of California, San Francisco, CA, May 10, 1996 (received for for review January 4, 1996)

ABSTRACT **The surfactant protein A (SP-A) gene was disrupted by homologous recombination in embryonic stem cells that were used to generate homozygous SP-A-deficient mice. SP-A mRNA and protein were not detectable in the lungs of SP-A(−/−) mice, and perinatal survival of SP-A(−/−) mice was not altered compared with wild-type mice. Lung morphology, surfactant proteins B–D, lung tissue, alveolar phospholipid pool sizes and composition, and lung compliance in SP-A(−/−) mice were unaltered. At the highest concentration tested, surfactant from SP-A(−/−) mice produced the same surface tension as (+/+) mice. At lower concentrations, minimum surface tensions were higher for SP-A(−/−) mice. At the ultrastructural level, type II cell morphology was the same in SP-A(+/+) and (−/−) mice. While alveolar phospholipid pool sizes were unperturbed, tubular myelin figures were decreased in the lungs of SP-A(−/−) mice. A null mutation of the murine SP-A gene interferes with the formation of tubular myelin without detectably altering postnatal survival or pulmonary function.**

Surfactant protein A (SP-A) is an abundant, phospholipid-associated protein in pulmonary surfactant. Murine SP-A is encoded by a single gene located on chromosome 14, at a site syntenic with the SP-A locus on chromosome 10 in humans (1). SP-A is synthesized and secreted primarily by type II and bronchiolar cells in the respiratory epithelium. In the alveolus, SP-A forms large oligomers and is closely associated with tubular myelin, the major extracellular form of surfactant (for a review, see ref. 2). SP-A contains a 10-kDa collagen-like amino-terminal domain and a globular carboxyl-terminal domain with structural homology to SP-D, mannose binding protein, C1q, and other members of the collectin family of mammalian lectins (3). Various functions related to surfactant have been ascribed to SP-A, based primarily on *in vitro* findings, which include enhancing phospholipid uptake (4), inhibiting surfactant secretion by isolated type II epithelial cells (5, 6), contributing to tubular myelin formation (7), enhancing surfactant spreading, stabilizing phospholipid mixtures (8) and conferring resistance to protein mediated inactivation of surfactant (9). Evidence has also accumulated that supports a role for SP-A in host defense. SP-A binds and increases the uptake of a variety of bacterial and viral pathogens by alveolar macrophages, activates alveolar macrophage metabolism, and enhances the uptake of bacterial pathogens by both macrophages and monocytes *in vitro* (10–13). In spite of the extensive *in vitro* evidence that SP-A is involved in surfactant homeostasis and function, there is little direct evidence that SP-A plays a critical role in surfactant function *in vivo*. To test the role of SP-A *in vivo*, the mouse SP-A gene was disrupted by homologous recombination in embryonic stem cells to produce mice lacking SP-A.

The publication costs of this article were defrayed in part by page charge payment. This article must therefore be hereby marked "*advertisement*" in accordance with 18 U.S.C. §1734 solely to indicate this fact.

MATERIALS AND METHODS

Generation of Null Mutant Mice. A 129J genomic library packaged in λ DASH II (Promega), kindly provided by Marcia Shull (University of Cincinnati), was screened to isolate the murine SP-A gene locus. Partial restriction endonuclease maps and partial sequence analysis of the 129J mouse genomic SP-A gene were highly homologous to the previously published gene from strain DBA2J (14). A 3.6-kb *Hin*dIII fragment of the murine SP-A gene was cloned into Puc18. The murine SP-A gene fragment digested with *Nco*I at positions 795 and 1049, and the *Hin*dIII/*Xho*I fragment containing pGKneoBPA were converted to blunt ends with Klenow fragment. pGKneoBPA was cloned between these positions to replace portions of exons 3 and 4 and intron 3. Orientation of pGKneoBPA was confirmed by *Pst*I restriction endonuclease digestion. Herpes simplex virus–thymidine kinase (HSV-TK) was cloned into the Puc18 *Nde*I site 3′ to pGKneoBPA insert. The targeted SP-A gene was prepared as a *Sal*I fragment for electroporation into embryonic stem (ES) cells.

ES cells (clone E14.1) generated from 129 ola mice were grown on neomycin-resistant mouse embryonic fibroblast feeder layers. Using ≈20 μg of the SP-A targeting construct, about 2×10^7 of the cells were electroporated. Targeted ES cells were selected by culture in G418 (150 μg/ml) and gancyclovir (2 μM). Targeted cells were identified by digestion of genomic DNA with *Eco*RI, *Ssp*I, or *Bam*HI and analyzed separately with two probes outside of the insert (probe 1 from positions 4028–4618 and probe 2 from positions 2215–3481) and a third internal probe (positions 769–2297) (see Fig. 1). Clone 87, a rapidly proliferative, undifferentiated ES cell clone, was microinjected into C57/Bl6 host blastocysts. Chimeric males were bred to NIH Swiss black females. Agouti offspring were screened for germ-line transmission of the targeted mutation by Southern blot analysis of *Ssp*I endonuclease digested tail DNA using the 1.2-kb *Hin*dIII fragment as probe (see Fig. 1). F1 heterozygous mice were bred to establish a colony of SP-A(+/+), SP-A(+/−), and SP-A(−/−) mice.

Immunohistochemistry, Western Blotting, and Northern Blotting. Lungs from adult SP-A(+/−), (−/−), and (+/+) mice were immunostained for SP-A, proSP-B, and proSP-C using guinea pig anti-rat polyclonal SP-A and rabbit polyclonal proSP-B and proSP-C antiserum as described (15–17). Lungs

Abbreviations: ES cells, embryonic stem cells; Sat PC, saturated phosphatidylcholine.

†To whom reprint requests should be addressed at: Children's Hospital Medical Center, Division of Pulmonary Biology, The Children's Hospital Research Foundation, 3333 Burnet Avenue, Cincinnati, OH 45229-3039.

§Present address: Department of Environmental Medicine, University of Rochester, Rochester, NY 14642.

were prepared by inflation fixation and embedded in paraffin before sectioning. For Western blot analysis of lung homogenates, mice were euthanized under protocols approved by the Institutional Animal Use and Care Committee. Lungs were homogenized in 10 mM Tris·HCl (pH 7.4), 0.25 M sucrose, 2 mM EDTA, 1 mM phenylmethylsulfonyl fluoride, 10 μM leupeptin, and 10 μM pepstatin A and centrifuged at 250 × *g* for 10 min at 2°C. Supernatants were centrifuged at 120,000 × *g* for 18 hr and the pellet resuspended in homogenizing buffer (minus sucrose) and subjected to SDS/PAGE on 10–27% gradient gels and transblotted to polyvinylidene difluoride (Bio-Rad) membranes, then blocked with 10 mM Tris·HCl (pH 7.4), 0.15 M NaCl, 0.1% Tween 20 (TBS-T) containing 5% bovine serum albumin. Blots were incubated with the anti-surfactant protein antisera described above or with anti SP-D kindly provided by E. Crouch (St. Louis, MO). Blots were rinsed and an appropriate horseradish-peroxidase-conjugated secondary antibody (Calbiochem) was added for 4 hr. Blots were rinsed and developed using ECL detection reagents (Amersham). Immunoreactive bands were identified by exposing blots to XAR film (Kodak). Where indicated, the polyvinylidene difluoride membrane was stripped using 62.5 mM Tris·HCl (pH 6.8), 2% SDS, and 0.1 M 2-mercaptoethanol, and reanalyzed using another primary antiserum. RNA isolation, Northern blot analyses, and S1 nuclease analyses were performed as described (14, 18, 19).

Pressure–Volume Curves. Lung compliance was measured in SP-A(+/+), (+/−), and (−/−) mice. Mice were injected i.p. with sodium pentobarbital (200 mg/kg) and placed in a chamber containing 100% O_2 to completely deflate the lungs. A catheter (24 g) was inserted into the trachea and connected to a silicon pressure sensor (X-ducer; Motorola, Phoenix, AZ). The chest wall and diaphragm were opened, and the lungs were inflated with air in small increments (0.1 ml every 20–30 s) to a maximal pressure of 25 cm H_2O. Lungs were deflated in stepwise fashion. Airway opening pressure and lung volume were recorded at each inflation and deflation increment. All measurements were completed within 15 min. Pressure–volume curves from each animal were used to assess lung compliance, defined as the slope of the linear region of the deflation curve where pressure ranged from −10 to 10 cm H_2O. Specific lung compliance was calculated as lung compliance divided by lung volume at 25 cm H_2O. The hysteresis ratio was determined as described (20), using software kindly provided by Gary S. Huvard (Huvard Research and Consulting, Chesterfield, VA). Differences among animals were evaluated by comparing lung compliances, specific lung compliances, hysteresis ratios, and lung volumes at 25 cm H_2O by one-way analysis of variance.

Electron Microscopy. Lungs from each of two SP-A-deficient (−/−) and two wild-type (+/+) mice were inflation fixed and prepared for electron microscopy as described (19). Ultrathin sections from 4–6 different blocks, representing both proximal and distal portions of the lung, were examined for secreted forms of surfactant phospholipid and type II cell morphology. Five randomly selected contiguous fields (equivalent to 19,845 μm^2) from each section were then scored at a magnification of 80,000 for the presence of tubular myelin. A total of 40 fields from the wild-type mice (158,760 μm^2) and 70 fields from the SP-A-deficient mice (277,830 μm^2) were examined to determine the relative abundance of tubular myelin in these samples.

Alveolar Lavage and Surfactant Characterization. Mice were injected i.p. with pentobarbital to achieve deep anesthesia, and the distal aorta was cut to exsanguinate each animal. For alveolar lavage, the chest of the animal was opened, a 20 g blunt needle was tied into the proximal trachea and five 1 ml aliquots of 0.9% NaCl were flushed into the lungs and withdrawn by syringe three times for each aliquot. The recovered lavage was pooled and the volume measured. The amount of saturated phosphatidylcholine (Sat PC) recovered by alveolar lavage was measured by extracting an aliquot of each alveolar lavage with chloroform/methanol (2:1), followed by treatment of the lipid extract with OsO_4 in carbon tetrachloride and alumina column chromatography according to Mason *et al.* (21). Phosphorus in Sat PC was measured by the Bartlett assay (22). Lung tissue after alveolar lavage was homogenized in saline and an aliquot was extracted and analyzed for Sat PC content. For measurements of phospholipid composition, chloroform/methanol extracts of alveolar lavages of individual mice were used for two-dimensional thin-layer chromatography (23). The spots were visualized with iodine vapor, scraped, and assayed for phosphorus content.

Surface Tension Measurements. Alveolar lavages were collected as above from 7- to 8-week-old mice by a series of five sequential lavages. Because surface tension measurements were made in the presence and absence of Ca^{2+}, separate pooled lavages were recovered using 0.9% NaCl or a calcium containing buffer (0.01 M Tris·HCl/0.0025 M $CaCl_2$/0.001 M $MgSO_4$/0.0001 M EDTA/0.15 M NaCl, pH 7.0). NaCl (0.9%) or the Ca^{2+} containing buffer was used for all subsequent processing and surface tension measurements. Surfactant was isolated by separating large aggregate and small aggregate fractions by centrifugation as described (24). The alveolar lavages were centrifuged at 40,000 × *g* for 15 min and the pellet was suspended in 0.9% NaCl or Ca^{2+} buffer and centrifuged again at 40,000 × *g* for 15 min. The surfactant pellet was suspended in a small amount of 0.9% NaCl or Ca^{2+} buffer. Sat PC in aliquots of large and small aggregate surfactant were measured and the percentage of large aggregate surfactant in alveolar lavage was calculated. The minimum surface tension was measured with a Wilhelmy balance with a platinum

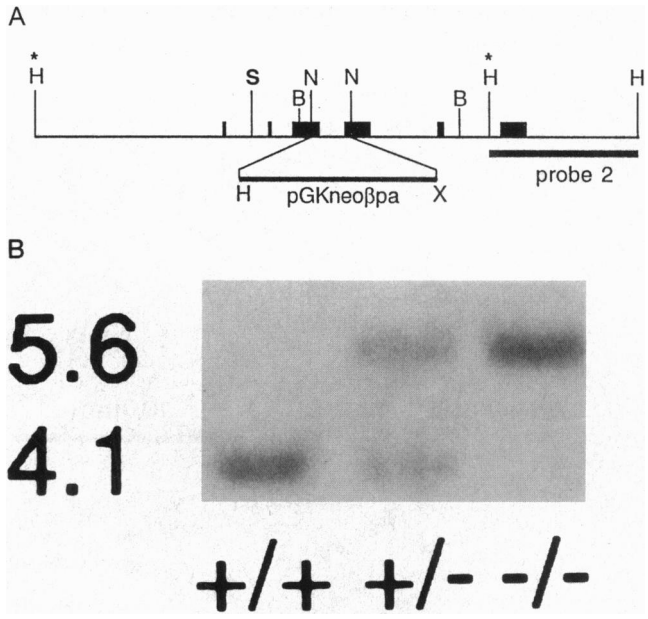

FIG. 1. SP-A locus targeting construct. (*A*) The top line (≈4.8 kb) depicts the mouse SP-A locus (14) with exons represented as boxes. Only the translated portion of exon 6 is depicted. pGKneoBPA was inserted into the 3′ terminus of exon 3 and 5′ terminus of exon 4, deleting those portions of the exons and intron 3. Pertinent restriction endonuclease sites and the position of probe 2 are depicted. Probe 1 (not shown) was used with *Eco*RI digestions, probe 2 (shown) with *Ssp*I, and probe 3 was the 1.5-Kb *Bam*HI fragment. The targeting construct was the modified *Hin*dIII fragment marked with asterisks. H, *Hin*dIII; S, *Ssp*I; B, *Bam*HI; N, *Nco*I. (*B*) Southern blot of genomic DNA probed with probe 2 following *Ssp*I digestion. The 4.1-kb *Ssp*1 band is the normal allele and the 5.6-kb *Ssp*I band is the targeted allele. Wild type (+/+), heterozygous (+/−), and homozygous (−/−) are depicted below the lanes.

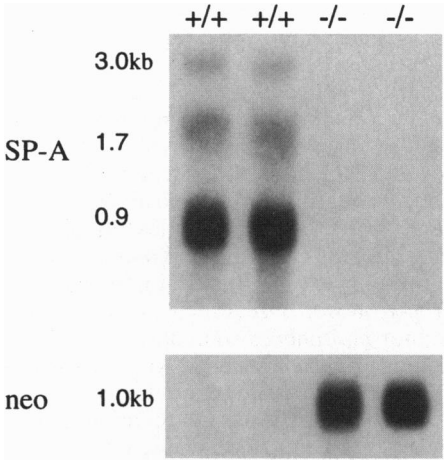

FIG. 2. SP-A mRNA in wild-type and SP-A(−/−) mice. Total lung RNA was probed with ^{32}P-labeled SP-A or neomycin probes. Genotype is depicted above the lanes. Size (in kb) of the expected mRNA bands are noted on the left. The data are representative of Northern blot analysis of lung RNA from five separate mice of both genotypes.

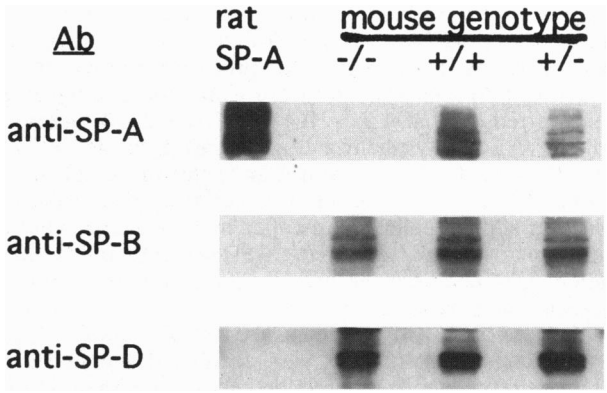

FIG. 3. Immunoblot of SP-A, proSP-B and SP-D in lung homogenates. Lung homogenates were prepared from SP-A(+/+), SP-A(+/−), and SP-A(−/−) mice, subjected to SDS/PAGE, and blotted as described. Antibody (Ab) is noted on the left; genotype is marked above the lanes. SP-A (34 kDa), proSP-B (≈42 kDa), and SP-D (≈43 kDa) are noted. Data are representative of two to five separate experiments. Rat SP-A was included in the gel as control.

dipping plate using 3 min area cycling from 64 cm^2 to 12.8 cm^2 at a temperature of 37°C (25). Surfactant was diluted in 35 ml 0.9% NaCl or Ca^{2+} buffer to a concentration of 0.005 μmol Sat PC/ml and, after each surface tension measurement, increments of 0.005 μmol Sat PC were added to maximum concentration of 0.025 μmol Sat PC/ml. The surfactant suspension was mixed after each surfactant addition, and surface compression was started 20 sec later. The surface tension-area loops overlapped by the third or fourth compression cycle and minimum surface tension on fourth cycle is reported.

RESULTS

Southern blot and partial restriction and sequence analysis of the 129J murine genomic SP-A locus demonstrated that SP-A was encoded by a single gene that was indistinguishable from the murine SP-A gene described in strain DBA/2J (14). The 129J genomic clone was used to prepare a targeting construct as depicted in Fig. 1. Insertion of pGKneoBPA deleted a portion of exon 3, intron 3, and a portion of exon 4 (from position 795-1049). Although the resulting allele maintains transcriptional start sites, the pGKneoBPA insert provides a strong competing start site and polyadenylylation signal and removes the splice signals of intron 3. A targeted ES cell clone

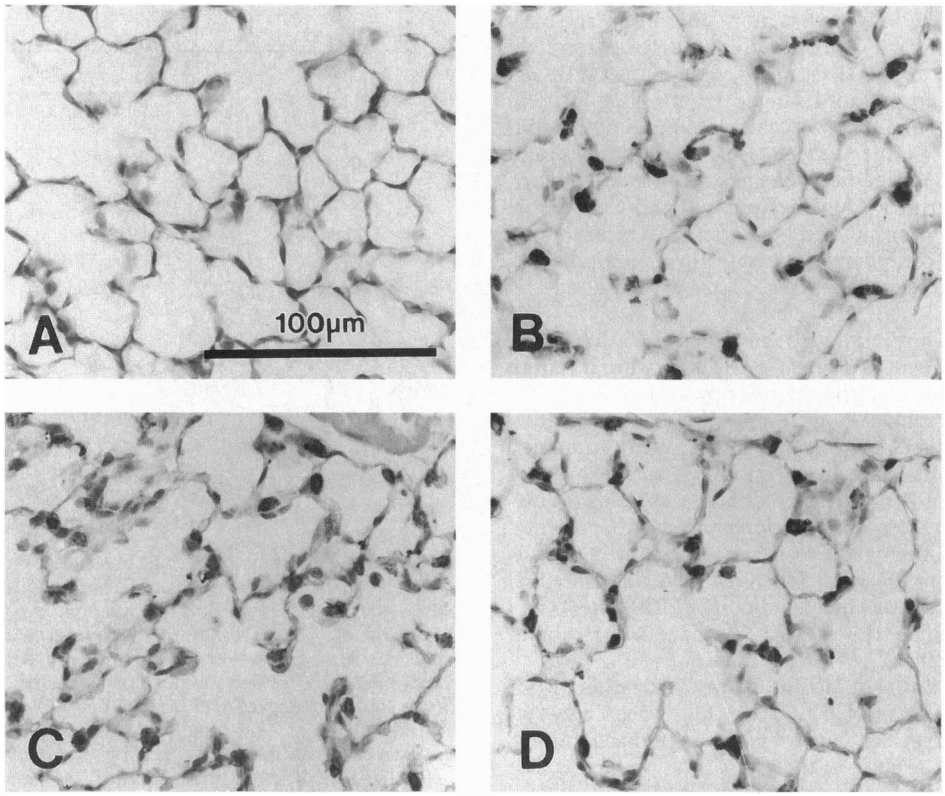

FIG. 4. Immunohistochemistry of surfactant proteins in SP-A(−/−) mice. Lung sections were stained for SP-A (*A* and *C*) and SP-B (*B* and *D*) from SP-A(−/−) (*A* and *B*) or SP-A(+/+) (*C* and *D*) as described. Histology and immunostaining of SP-A(+/−) mice were similar to those in wild-type mice (data not shown). (Bar = 100 μm.)

was microinjected into mouse blastocysts that were transferred to surrogate dams. Chimeric males were bred to NIH Swiss black females. Heterozygous F1 offspring were bred to produce SP-A (+/+), (+/−), and (−/−) mice. The distribution of genotype among the initial 246 offspring was 67 (+/+), 128 (+/−), 51 (−/−) for a ratio of 0.54/1.04/0.42, approximating that predicted by normal Mendelian inheritance. Heterozygous and homozygous SP-A gene targeted mice were not distinguishable from normal littermates in growth and reproduction. A pair of SP-A(−/−) mice have been maintained in microisolator containment for more than 8 months without evidence of ill health.

SP-A mRNA was not detectable in the lungs of the homozygous gene targeted animals by Northern blot analysis (Fig. 2). Using S1 nuclease analysis, the abundance of SP-A mRNA was reduced by approximately half in the heterozygous SP-A gene targeted animals (not shown). SP-A protein was not detected in lung homogenates from homozygous mice (−/−; see Fig. 3). There was a reduction of SP-A protein in the heterozygous SP-A gene targeted animals compared with control littermates. SP-B and SP-D protein were not altered in SP-A(+/−) or SP-A(−/−) mice (Fig. 3). ProSP-C protein was also not altered (data not shown).

Histochemical analysis of the lungs from the SP-A(−/−) mice revealed no abnormalities of lung structure and no evidence of inflammation. Immunohistochemical staining demonstrated the lack of SP-A in alveolar type II cells of SP-A(−/−) mice (Fig. 4*A*). The distribution of type II cells and abundance of surfactant protein proSP-B was also unchanged in SP-A(−/−) mice (Fig. 4*B*). The distribution of proSP-C was unchanged (not shown).

Composition of phosphatidylcholine, phosphatidylglycerol, phosphatidylinositol, phosphatidylethanolamine, and sphingomyelin was not altered in alveolar lavages or lung tissue of SP-A(−/−) mice (Fig. 5). Lung volumes and compliance of the SP-A(−/−) mice were similar to wild-type SP-A(+/+) littermates (Table 1). The percentages of surfactant isolated as large aggregates in alveolar lavages were similar for both groups and were 34.0 ± 2.9% of the total Sat PC (n = 10 pools of seven animals each) for SP-A(+/+) mice and 34.4 ± 2.7% (n = seven pools of seven animals each) for SP-A(−/−) mice. Independent of isolation or measurement of minimum surface tension in the presence or absence of Ca^{2+}, surfactant from

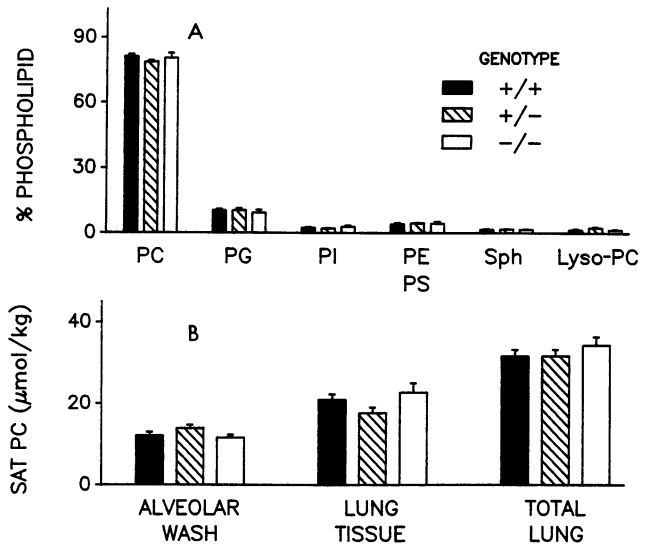

FIG. 5. Phospholipid composition. (*A*) Phospholipid composition was measured in alveolar lavage and lung homogenates from SP-A(+/+), SP-A(+/−), and SP-A(−/−) mice. Values are mean ± SEM. (*B*) Sat PC was determined in the alveolar washed lung tissue (mean ± SEM; n = 4–6 determinations).

Table 1. Lung volumes and compliance

Genotype	Lung volume	Compliance*	Hysteresis ratio
+/+ (n = 7)	28 ± 3	0.091 ± 0.008	0.383 ± 0.031
+/− (n = 3)	26 ± 5	0.058 ± 0.008	0.439 ± 0.024
−/− (n = 9)	26 ± 3	0.074 ± 0.008	0.384 ± 0.024

Lung volume is expressed as μl contained in the lung at 25 cm H_2O divided by body weight. All values were compared by one way analysis of variance and are expressed as mean ± SEM.

*Compliance was determined by calculating the slope of the deflation pressure–volume curve between −10 and +10 cm of water divided by lung volume.

SP-A(+/+) and SP-A(−/−) mice had low minimum surface tensions at a bulk phase concentration of 0.025 μmol Sat PC/ml (Fig. 6). Surface tensions for surfactant from SP-A(−/−) mice tended to be higher at lower concentrations in the presence of Ca^{2+} and were significantly higher in the absence of Ca^{2+} than for surfactant from SP-A(+/+) mice.

To determine if the morphology of type II cells or tubular myelin was altered, lungs were prepared for electron microscopy. The morphology of type II epithelial cells in SP-A(−/−) was identical to that of wild-type animals (Fig. 7*A*). While tubular myelin structures were readily detected in wild-type littermates, tubular myelin figures were markedly deficient in the SP-A(−/−) mice. Of 70 fields examined from two (−/−) mice, only two small tubular myelin figures were detected; one is shown in Fig. 7*B*. In contrast, 40 fields examined from two (+/+) mice revealed 15 large tubular myelin figures and one representative figure is shown in Fig. 7*C*. The preponderant form of alveolar lipids in SP-A(−/−) mice were lamellated and membranous lipid forms lacking the dense, highly geometric forms characteristic of tubular myelin Fig. 7*D*).

DISCUSSION

SP-A deficiency in homozygous SP-A gene targeted mice led to production of surfactant with reduced surface tension

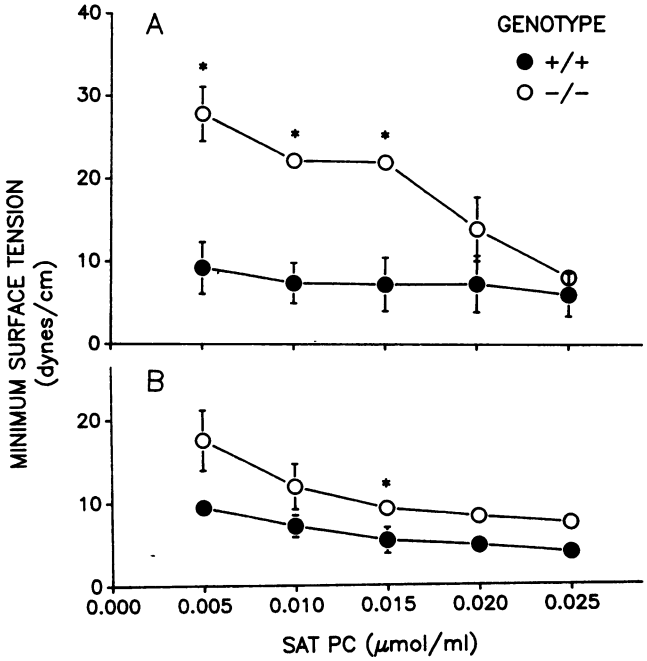

FIG. 6. Minimum surface tensions. Surfactants recovered from 10 mice for each of three pooled samples isolated in the presence or absence of Ca^{2+} from SP-A(+/+) and SP-A(−/−) mice were used for surface tension measurements. Measurements were made in the absence (*A*) or presence (*B*) of 2.5 mM Ca^{2+}. Values are for three measurements at each concentration (mean ± SEM). *, $P < 0.05$ relative to SP-A(+/+) mice.

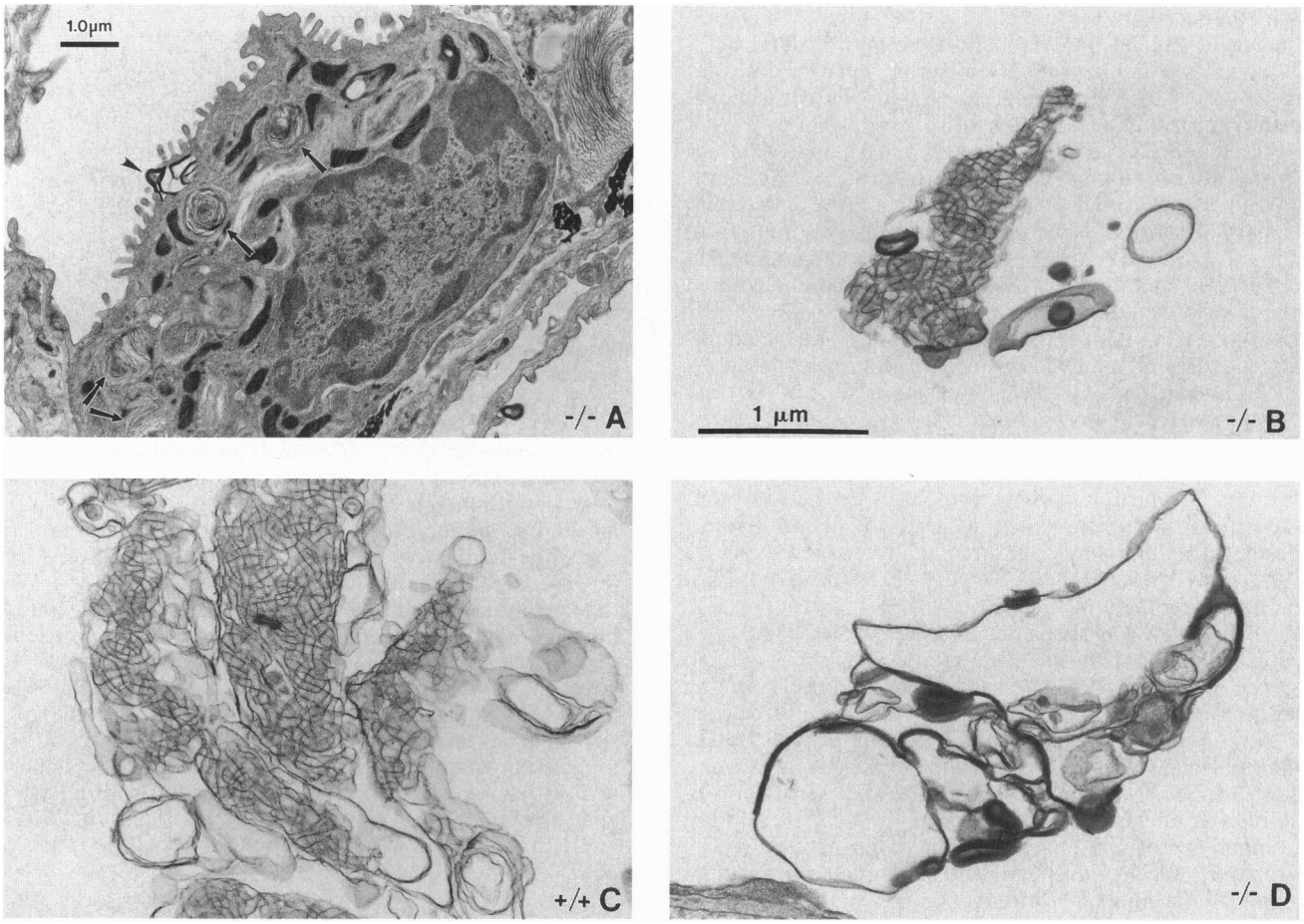

FIG. 7. Ultrastructural analysis of type II alveolar cells and alveolar surfactant in SP-A-deficient mice. Lung tissue was obtained from adult mice and prepared for electron microscopy as described. (A) Intact, mature lamellar bodies (arrows) were readily detected in the apical cytoplasm of type II alveolar cells from SP-A-deficient mice. Surfactant secretion was also observed at the apical cell surface (arrowhead). (Bar = 1.0 μm.) (*B*) One of two tubular myelin figures detected in SP-A(−/−) mice. (*C*) One of 15 tubular myelin figures from SP-A(+/+) mice. (*D*) A representative lung section from SP-A(−/−) mice showing membranous forms of phospholipid that lacked the more highly ordered, geometric organization characteristic of tubular myelin. (*B–D* were printed at the same magnification; bar in *B* is 1.0 μm.)

lowering properties at low phospholipid concentrations without altering levels of intracellular/extracellular surfactant phospholipids. The abundance of tubular myelin figures *in vivo* was reduced but the abundance of surfactant proteins B, C, and D were unaltered. SP-A-deficient mice have no apparent breeding or survival abnormalities when housed in well-controlled, pathogen-free cages in the vivarium. These findings demonstrate a phospholipid concentration dependence on surface tension reducing properties in the absence of SP-A and the importance of SP-A in the formation of tubular myelin, the characteristic extracellular form of surfactant. The findings of small tubular myelin figures in the (−/−) mice may suggest that figures are transiently formed but not stabilized in the absence of SP-A. Alternatively, there may be very low levels of SP-A, below detectability, that are sufficient to lead to formation of markedly reduced numbers of tubular myelin figures.

The disruption of the SP-A locus led to a lack of detectable SP-A mRNA and protein in the SP-A(−/−) mice and was not associated with changes in surfactant proteins SP-B, proSP-C, or SP-D. These findings support previous data suggesting that surfactant protein genes are independently regulated. As in the SP-B null mutant mice (19), wherein SP-A and -C mRNAs were unaltered, the regulation of surfactant protein genes does not appear to be under compensatory regulatory signals related to deficiency of SP-A or SP-B.

Consistent with the finding that the concentration of SP-B and -C in lavage from the SP-A(−/−) mice were unaltered, the distribution and abundance of immunostaining for surfactant proteins proSP-B and proSP-C were also not different from controls. Immunohistologic analysis demonstrated the complete absence of SP-A in the alveoli of SP-A(−/−) and a reduced amount in SP-A(−/+) mice, demonstrating that the level of SP-A does not alter the steady-state levels of SP-A mRNAs and protein. In spite of the reduction of SP-A in SP-A(+/−) and the absence of SP-A in SP-A(−/−) mice, the gene targeted animals continue to survive (at least 8 months) with no apparent illness, in viral free housing with controlled humidity and temperature and access to unlimited food and water.

SP-A has been postulated to play an important role in the regulation of surfactant phospholipid levels by inhibiting phospholipid secretion of type II cells and enhancing the reuptake of surfactant phospholipids *in vitro* (4–6). However, in the present study, there were no detectable alterations in intracellular or extracellular pool sizes or composition of surfactant phospholipids from SP-A(−/−) mice suggesting that SP-A does not determine the abundance of the major phospholipid classes of surfactant *in vivo*. Alternatively, counterregulatory measures, independent of surfactant proteins or pool sizes, may contribute to the maintenance of steady-state phospholipid concentrations in the intracellular and extracellular spaces in the SP-A(−/−) mice.

At the highest bulk phase concentration tested on the Wilhelmy surface balance, surfactant from the SP-A(−/−) mice yielded the same low surface tension as surfactant from

control mice. At lower surfactant concentrations, minimum surface tensions are higher for surfactant from the SP-A(−/−) mice. These results are consistent with the lack of apparent abnormalities in lung compliance in the SP-A(−/−) mice because surfactant concentration is very high in the continuous thin film of fluid that is the alveolar lining layer (26). By extrapolation from estimates for the human, the adult mouse lung would have an alveolar fluid volume of 40 μl and a surface area of about 0.1 m^2 (27, 28). The concentration of Sat PC in this alveolar fluid would be on the order of 10 μmol/ml, a value more than three orders of magnitude higher than tested on the surface balance. Phospholipids in the presence of SP-B and SP-C without SP-A were previously shown to spread normally (29). The lack of altered surfactant function in the SP-A(−/−) mice is further supported by the observed normal lung compliance (Table 1).

Surfactant homeostasis is mediated by complex synthetic, secretory, and catabolic processes that include recycling and catabolism of surfactant phospholipids by respiratory epithelial cells and catabolism by alveolar macrophages. The findings that steady-state phospholipid concentrations were unaltered in the SP-A-deficient mice are consistent with previous findings demonstrating the lack of effect of SP-A on clearance of surfactant mixtures *in vivo*. In the neonatal rabbit, the clearance of surfactant lipids in the airspace was identical in the presence or absence of exogenous SP-A (30). In contrast, at nonphysiologic concentrations of phospholipids, there is a difference in surface tension lowering properties of isolated surfactant. These data suggest that in conditions where phospholipid concentrations were altered *in vivo*, SP-A could play a critical role in maintenance of surface tension reducing properties. Such conditions may occur with infections, toxic, or immunologic injury to the lung epithelium. This concept is supported by *in vitro* evidence that SP-A protects surfactant from protein inactivation (9) and binds and enhances uptake of microbial pathogens (10–13). In future studies it will be important to determine pulmonary function in SP-A-deficient mice following infectious or toxic injury to determine the full physiologic functions of SP-A.

We thank Dr. E. Crouch for the gift of an anti-SP-D antibody and Drs. John Duffy and Tom Doetschman for assistance in generating gene targeted chimeric mice. This work was supported by Grant HL28623 from the National Institutes of Health (T.R.K. and J.A.W.), by the Cystic Fibrosis Foundation, and by the Program of Excellence Molecular Biology (Grants HL41496 and HD11932).

1. Moore, K. J., D'Amore-Bruno, M. A., Korfhagen, T. R., Glasser, S. W., Whitsett, J. A., Jenkins, N. A. & Copeland, N. G. (1992) *Genomics* **12,** 388–393.
2. Hawgood, S. & Clements, J. A. (1990) *J. Clin. Invest.* **86,** 1–6.
3. White, R. T., Damm, D., Miller, J., Spratt, K., Schilling, J., Hawgood, S., Benson, B. & Cordell, B. (1985) *Nature (London)* **317,** 361–363.
4. Wright, J. R., Wager, R. E., Hawgood, S., Dobbs, L. & Clements, J. A. (1987) *J. Biol. Chem.* **262,** 2888–2894.
5. Dobbs, L. G., Wright, J. R., Hawgood, S., Gonzales, R., Venstrom, K. & Nellenbogen, J. (1987) *Proc. Natl. Acad. Sci. USA* **84,** 1010–1014.
6. Rice, W. R., Ross, G. F., Singleton, F. M., Dingle, S. & Whitsett, J. A. (1987) *J. Appl. Physiol.* **63,** 692–698.
7. Suzuki, Y., Fujita, Y. & Kogishi, K. (1989) *Am. Rev. Respir. Dis.* **140,** 75–81.
8. Hawgood, S., Benson, B. J. & Hamilton, R. L. J. (1985) *Biochemistry* **24,** 184–190.
9. Cockshutt, A. M., Weitz, J. & Possmayer, F. (1990) *Biochemistry* **29,** 8424–8429.
10. Gaynor, C., McCormack, F. X., Voelker, D. R. & Schlesinger L. (1995) *J. Immunology* **155,** 5343–5351.
11. van Iwaarden, J. F., Pikaar, J. C., Storm, J., Brouwer, E., Verhoef, J., Oosting, R. S., Van Golde, L. M. G. & Van Strijp, J. A. G. (1994) *Biochem. J.* **303,** 407–411.
12. Tenner, A. J., Robinson, S. L., Borchelt, J. & Wright, J. R. (1989) *J. Biol. Chem.* **264,** 13923–13928.
13. Pison, U., Max, M., Neuendank, A., Weibbach, S. & Pietchmann, S. (1994) *J. Clin. Invest.* **24,** 586–599.
14. Korfhagen, T. R., Bruno, M. D., Glasser, S. W., Ciraolo, P. J., Whitsett, J. A., Lattier, D. L., Wikenheiser, K. A. & Clark, J. C. (1992) *Am. J. Physiol.* **263,** L546–L554.
15. Slavkin, H. C, Johnson, R., Oliver, P., Bringas, P., Don-Wheeler, G., Mayo, M. & Whitsett, J. A. (1989) *Differentiation* **41,** 223–236.
16. Khoor, A., Stahlman, M. T., Gray, M. E. & Whitsett, J. A. (1994) *J. Histochem. Cytochem.* **42,** 1187–1199.
17. Vorbroker, D. K., Profitt, S. A., Nogee, L. M. & Whitsett, J. A. (1995) *Am. J. Physiol.* **268,** L647–L656.
18. Dranoff, G., Crawford, A. D., Sadelain, M., Ream, B., Rashid, A., Bronson, R. T., Dickersin, G. R., Bachurski, C. J., Mark, E. L., Whitsett, J. A. & Mulligan, R. C. (1994) *Science* **264,** 713–716.
19. Clark, J. C., Wert, S. E., Bachurski, C. J., Stahlman, M. T., Stripp, B. R., Weaver, T. E. & Whitsett, J. A. (1995) *Proc. Natl. Acad. Sci. USA* **92,** 7794–7798.
20. Nardell, E. A. & Brody, J. S. (1982) *J. Appl. Physiol.* **53,** 140–148.
21. Mason, R. J., Nellenbogen, J. & Clements, J. A. (1976) *J. Lipid Res.* **17,** 281–284.
22. Bartlett, G. R. (1959) *J. Biol. Chem.* **234,** 466–468.
23. Jobe, A. H., Kirkpatrick, E. & Gluck, L. (1978) *J. Biol. Chem.* **253,** 3810–3816.
24. Ikegami, M., Ueda, T., Hull, W., Whitsett, J. A., Mulligan, R. C., Dranoff, G. & Jobe, A. H. (1996) *Am. J. Physiol.* **270,** L650–L658.
25. Ikegami, M., Jobe, A. & Glatz, T. (1981) *J. Appl. Physiol.* **51,** 306–312.
26. Bastacky, J., Lee, C. Y. C., Goerke, J., Koushafar, H., Yager, D., Kenaga, L., Speed, T. P., Chen, Y. & Clements, J. A. (1995) *J. Appl. Physiol.* **79,** 1615–1628.
27. Rannard, S. I., Basset, G., Lecossier, D., O'Donnell, K. M., Pinkston, P., Martin, P. G. & Crystal, R. G. (1986) *J. Appl. Physiol.* **60,** 532–538.
28. Weibel, E. R. (1987) *Annu. Rev. Physiol.* **49,** 147–159.
29. Ross, G. F., Notter, R. H., Meuth, J. & Whitsett, J. A. (1986) *J. Biol. Chem.* **261,** 14283–14291.
30. Ikegami, M., Lewis, J. F., Tabor, B., Rider, E. D. & Jobe, A. H. (1992) *Am. J. Physiol.* **262,** L765–L772.